# Reaction-Sheet Jump Conditions in Premixed Flames

J.W. Dold, R.W. Thatcher, A.A. Shah

Mathematics Department, UMIST, Manchester M60 1QD, U. K.
< John.Dold@umist.ac.uk >

**Abstract**

The fundamental differences between the leading-order jump conditions, often assumed at a flame sheet in combustion theory, and the actual effect of a chemical reaction that satisfies Arrhenius kinetics with a finite activation temperature, need to be understood. These differences are "higher order" in terms of a large activation temperature analysis. However, they do provide a quantitative estimate of the errors that are inherent in adopting only the leading order version and they can indicate qualitative changes that may occur at finite activation temperatures in some cases. This paper derives two orders of asymptotic correction to the jump conditions normally used in describing premixed laminar combustion. An example involving steady, non-adiabatic flame-balls shows that the accepted asymptotic picture is limited to unusually large Zel′dovich numbers.

## 1 Introduction

When studying premixed flames that involve a thermally sensitive, exothermic, one-step reaction of the form

$$\nu_{\mathtt{F}}\mathtt{F} + \nu_{\mathtt{X}}\mathtt{X} \rightarrow \mu_{\mathtt{P}}\mathtt{P}$$

a common practice in combustion theory is to assume that all chemistry takes place on an infinitesimally thin free boundary, or sheet of reaction, at a rate that depends only on temperature (see [1]–[3] for suitable examples). This leads to considerable simplification in the model and its analysis, while remaining physically relevant, since thermal sensitivity, of the rate at which reactants are consumed and heat is released, is normally the single most important practical feature of the chemistry.

However, it is important also to ascertain what effects are being neglected when adopting this form of model, even if only to confirm that the effects are small. This paper examines the jump conditions that may be used across a flame sheet, as a systematic asymptotic reduction from a one-step Arrhenius description of the chemistry for large activation temperature. At higher orders, there is a dependence on curvature, speed of gas flow through the sheet and normal temperature gradient in the burnt gases.

In cases where the activation temperature is large enough and the temperature at the reaction sheet undergoes any form of change, either in time or as parameters change, these higher order effects are likely to be unimportant, qualitatively and quantitatively,

providing only very minor corrections. The strong thermal sensitivity of the reaction rate at high activation temperature is likely to overwhelm every other effect. However, in cases where there is very little change in temperature at the reaction sheet, other influences may play a significant role. It is informative, anyway, to quantify the roles that curvature, propagation speed and conduction into the burnt gas, must play in modifying the jump conditions usually encountered at a reaction sheet.

Stability analyses, leading for example to the Sivashinsky equation [4] or describing the stability of flame balls [5]–[7], often involve a dispersion relation that covers two orders of magnitude, or more, in a perturbation parameter. By adopting only the leading order jump conditions at a flame sheet and assuming, as part of a model for the combustion, that these are correct to all orders of accuracy, there may therefore be some inconsistency. However, except possibly in some critical cases, higher order terms in the jump conditions probably would not alter the essential nature of the dispersion relation in any qualitatively important way.

While the use of jump conditions at a reaction sheet is extremely useful in examining analytically the structure, stability and behaviour of various forms of premixed flames, their use is less practical in carrying out numerical simulations of flames with one-step chemistry. The numerical implementation of a moving free-boundary problem, at which specific boundary conditions need to be satisfied, is much more problematic than the simulation of a chemical process that is spatially distributed, even if it only happens on a relatively small (but not infintesimally small) scale. The activation temperature used in any one numerical simulation must also then be fixed and, necessarily, finite.

Unexpectedly large differences can then arise between asymptotic predictions for large activation temperature, based on using jump conditions, and numerical observations at finite, albeit realistic, activation temperatures [7]. Higher order corrections to the jump conditions can be used to estimate these differences.

In this paper, we derive two orders of asymptotic correction to the jump conditions normally used in describing premixed laminar combustion. As an example of their utility, a comparison with numerical calculations of some steady, non-adiabatic flame balls illustrates the way in which high-order jump conditions can be used to predict the magnitude of Zel′dovich number that is needed to achieve reasonable agreement between asymptotic estimates and numerical results. In fact, the agreement is found to be even worse than predicted at all but inordinately high Zel′dovich numbers, although the high order jump conditions predict the onset and basic nature of the disagreement quite well.

# 2 Model

A dimensionless low Mach number model, that describes the one-step decomposition reaction $\mathtt{F} \rightarrow \mathtt{P}$ using an Arrhenius rate law, can be written as

$$\begin{aligned} F_t + \mathbf{v}\cdot\nabla F &= \tfrac{1}{\mathrm{Le}}\nabla^2 F - D\,\omega \\ T_t + \mathbf{v}\cdot\nabla T &= \nabla^2 T + Q D\,\omega \\ \omega &= F\exp\left(\theta/T_* - \theta/T\right) \end{aligned} \tag{1}$$

in which Le is the Lewis number of the reactant F, the scaled mass-fraction of which is represented by $F(t,\mathbf{x})$; $Q$ is a heat release parameter; $T_*$ is a suitably chosen dimensionless

reference temperature, that is typically close to the maximum value that can be estimated for the absolute temperature $T(t,\mathbf{x})$; and the velocity $\mathbf{v}(t,\mathbf{x})$ is a solution of the Navier-Stokes equations

$$\rho_t + \nabla\cdot(\rho\mathbf{v}) = 0, \quad \rho(\mathbf{v}_t + \mathbf{v}\cdot\nabla\mathbf{v}) + \nabla p = \rho\,\mathrm{Pr}\nabla\cdot\left(\nabla\mathbf{v} + (\nabla\mathbf{v})^{\mathrm{T}}\right) + \mathbf{g}$$

in which Pr is the Prandtl number and $\mathbf{g}$ is a vectorial form of Froude number, or a dimensionless gravitational vector. These equations are linked to the combustion equations (1) via the dimensionless form of the isobaric ideal gas law $\rho T = 1$, since the density $\rho(t,\mathbf{x})$ then changes as the temperature changes. Variations in absolute pressure, of the order of the square of the Mach number, are represented by the dimensionless hydrodynamic pressure $p(t,\mathbf{x})$. Only if the ideal gas law is replaced by a constant density model, $\rho \equiv 1$, is the velocity independent of any temperature changes [1]–[3].

When the activation temperature $\theta$ is large enough, the reaction-rate term $\omega$ is commonly considered only to act at an infinitely thin reaction sheet, or interface, $\mathbf{\Gamma} \subset \mathbb{R}^3$. The effect of the chemistry is then entirely summarised by jump conditions applied to $F$ and $T$ across the interface. For a suitably defined value of the Damköhler number $D$, namely $D = \delta^2\theta^2 Q^2/2\mathrm{Le}T_*^4$, the model then typically takes the form

$$\left.\begin{aligned} F_t + \mathbf{v}\cdot\nabla F &= \tfrac{1}{\mathrm{Le}}\nabla^2 F \\ T_t + \mathbf{v}\cdot\nabla T &= \nabla^2 T \end{aligned}\right\} \quad \text{for} \quad \mathbf{x} \notin \mathbf{\Gamma}$$
$$\left.\begin{aligned} [T] = [F] = F &= 0 \\ \tfrac{1}{\mathrm{Le}}[F_n] = -\tfrac{1}{Q}[T_n] &= \delta \mathrm{e}^{(\theta/T_*-\theta/T)/2} \end{aligned}\right\} \quad \text{at} \quad \mathbf{x} \in \mathbf{\Gamma} \tag{2}$$

in which $\partial_n = \widehat{\mathbf{n}}\cdot\nabla$ is the normal gradient, or spatial derivative in the direction to which a normal unit vector $\widehat{\mathbf{n}}$ points. The brackets, $[\,\cdot\,]$, denote the usual jump in value across the sheet of the contents of the brackets, being the value on the side of the interface to which $\widehat{\mathbf{n}}$ points minus the value on the opposite side. It is useful to think of $\widehat{\mathbf{n}}$ as pointing in the direction of propagation of the interface or, more generally, towards increasing values of $F$, and this convention will be adopted in this article.

The jump conditions in (2) state that $T$ and $F$ are continuous across the interface where the reactant concentration $F$ must also have the value zero. The jumps in $T_n$ and $F_n$ are linearly related to each other and take a value that is a nonlinear function of only the temperature at the interface. Since $\theta$ is large, they are also a highly sensitive function of temperature. On one side of the flame sheet the chemistry must be in equilibrium, $\omega = 0$, which is ensured in equations (1) by having $F \equiv 0$. On the other side, the temperature is typically far enough below $T_*$ for the value of $\omega$ to be transcendentally small as $\theta \to \infty$. Neglecting the reaction rate $\omega$ when $\mathbf{x} \notin \mathbf{\Gamma}$ is therefore quite reasonable when $\theta$ is large enough.

According to the model (2), premixed flames of various types (laminar flames or flameballs) are thus envisaged as having a structure in which all chemical reaction is concentrated around a narrow sheet, the interface $\mathbf{\Gamma}$, with reactant concentration and temperature determined by inert advective and diffusive processes away from the sheet. The approximation has been demonstrated to work well in examples that are too numerous to cite in this paper (see [1]–[3]).

# 3 Reaction sheet jump conditions

## 3.1 Temperature dependence of the jump conditions

A complete description of the temperature dependence in the jump conditions at the reaction sheet can be arrived at by selecting a particular form for the model problem (1) in which no other effects are present.

For this, we can consider a completely stationary, one-dimensional problem, with no flow, in which $F = F(x)$ and $T = T(x)$, only. Taking $F(-\infty) = 0$ and $T(-\infty) = \widehat{T}$, where the value of $\widehat{T}$ is within order $\theta^{-1}$ of $T_*$, equations (1) then reduce to the model equations and boundary conditions for $F$ and $T$

$$\tfrac{1}{\mathrm{Le}}F'' = -\tfrac{1}{Q}T'' = DF\exp\big(\theta\tfrac{T-T_*}{T_*T}\big) \quad \text{with} \quad \lim_{x\to-\infty} F = 0, \quad \lim_{x\to-\infty} T = \widehat{T}. \tag{3}$$

It can be noted that $(F,T) \equiv (0,\widehat{T}\,)$ provides an exact, constant solution, corresponding to complete chemical equilibrium. Also, the reaction rate term becomes transcendentally small as $\theta \to \infty$ when $F > 0$ and $T < \widehat{T} - O\big(\frac{\ln\theta}{\theta}\big)$. The second derivatives are then negligibly small so that $F$ and $T$ become linear in $x$ to exponential orders of accuracy. The change in slope between the constant and linear forms of behaviour (when $F = 0$ and when $F > 0$) is, of course, determined by the reaction-rate term.

Since $F \geq 0$ it follows that $F$, and also $T$, monotonically approach their values at $x = -\infty$. Thus $F'(-\infty) = T'(-\infty) = 0$ and the first equality in (3) can be integrated exactly to give $T = \widehat{T} - \frac{Q}{\mathrm{Le}}F$. Writing $\mathit{f}(x) = \theta\frac{Q}{\mathrm{Le}}F(x)\big/\widehat{T}^2$ it follows that

$$\mathit{f}'' = \tfrac{1}{2}k^2\mathit{f}\exp\Big(-\tfrac{\mathit{f}}{1-\mathit{f}\,\widehat{T}/\theta}\Big) \quad \text{with} \quad k^2 = 2\mathrm{Le}D\exp\Big(\tfrac{\theta(\widehat{T}-T_*)}{T_*\widehat{T}}\Big)$$

so that, since $\mathit{f}'$ is zero when $\mathit{f} = 0$

$$\begin{aligned}
\frac{\mathit{f}'^2}{k^2} &= \int_0^{\mathit{f}} z\exp\Big(-\tfrac{z}{1-z\widehat{T}/\theta}\Big)\mathrm{d}z = \int_0^{\frac{\mathit{f}}{1-\mathit{f}\,\widehat{T}/\theta}} \frac{u\mathit{e}^{-u}}{(1+u\widehat{T}/\theta)^3}\,\mathrm{d}u \\
&= \int_0^{\mathit{f}} z\mathit{e}^{-z}\Big(1 - z^2\tfrac{\widehat{T}}{\theta} - \big(z^3-\tfrac{1}{2}z^4\big)\tfrac{\widehat{T}^2}{\theta^2} - \big(z^4-z^5+\tfrac{1}{6}z^6\big)\tfrac{\widehat{T}^3}{\theta^3} + O\big(\theta^{-4}\big)\Big)\mathrm{d}z \\
&= 1-(1+\mathit{f})\mathit{e}^{-\mathit{f}} - 6\big(1-(1+\mathit{f}+\tfrac{1}{2}\mathit{f}^2+\tfrac{1}{6}\mathit{f}^3)\mathit{e}^{-\mathit{f}}\big)\tfrac{\widehat{T}}{\theta} + O\big(\theta^{-2}\big)
\end{aligned}$$

in which the second integral has an exact, but lengthy, expression in terms of exponential integral functions. When $\mathit{f}$ is strictly of order $\theta$, or $F > o(1)$, as $\theta \to \infty$, this exact solution for $\mathit{f}'^2/k^2$ defines a constant value for $\mathit{f}'$, to exponential orders of accuracy. Approximating this constant to algebraic orders (by expanding the exponential for large values of $\theta$ as indicated in the equation above, and finally letting $\mathit{f} \to \infty$) gives

$$\frac{\mathit{f}'^2}{k^2} = 1 - 6\tfrac{\widehat{T}}{\theta} + 36\tfrac{\widehat{T}^2}{\theta^2} - 240\tfrac{\widehat{T}^3}{\theta^3} + O\big(\theta^{-4}\big) = \exp\Big(-6\tfrac{\widehat{T}}{\theta}\Big) + O\big(\theta^{-3}\big)$$

after continuing the procedure in a straightforward way to the order of $\theta^{-3}$.

The values of $F'$ and $T'$ when $F > O\big(\frac{\ln\theta}{\theta}\big)$ can therefore be estimated as

$$\begin{aligned}
\tfrac{1}{\mathrm{Le}}F' = -\tfrac{1}{Q}T' &= \tfrac{\widehat{T}^2}{Q\theta}\sqrt{2\mathrm{Le}D}\exp\Big(\tfrac{\theta}{2}\tfrac{\widehat{T}-T_*}{T_*\widehat{T}} - 3\tfrac{\widehat{T}}{\theta} + O\big(\theta^{-3}\big)\Big) \\
&= \delta\tfrac{\widehat{T}^2}{T_*^2}\exp\Big(\tfrac{\theta}{2}\tfrac{\widehat{T}-T_*}{T_*\widehat{T}} - 3\tfrac{\widehat{T}}{\theta} + O\big(\theta^{-3}\big)\Big)
\end{aligned} \tag{4}$$

after setting $D = \delta^2\theta^2 Q^2/2\mathrm{Le}T_*^4$. By noting that $T_*$ needs to be chosen to be within order $\theta^{-1}$ of typical values of $\widehat{T}$, for order one changes in gradient to arise in the dimensionless scalings adopted in the model, it follows that the ratio $\widehat{T}^2/T_*^2$ must be asymptotically close to unity. Now extrapolating the values of $F$ and $T$ back to a point where $F$ would extrapolate to zero, and $T$ would extrapolate to $\widehat{T}$, this point identifies a location where the overall changes in $F$, $T$ and their gradients should behave as if they satisfied the jump conditions given in (2), in which the errors are of the order of $\theta^{-1}$. Using the expression given in (4) would reduce the errors to order $\theta^{-3}$, provided there were no other factors, apart from temperature, influencing the jump conditions.

## 3.2 Curvature, flow and unsteady effects at the flame-sheet

It is informative now to examine some of the other factors that are being neglected in adopting the flame sheet model (2). For this purpose, let us consider the slightly more simplified model

$$\begin{aligned} F_t + \mathbf{v}\cdot\nabla F &= \tfrac{1}{\mathrm{Le}}\nabla^2 F - \tfrac{\beta^2}{2\mathrm{Le}}\omega \\ \mathsf{T}_t + \mathbf{v}\cdot\nabla \mathsf{T} &= \nabla^2 \mathsf{T} + \tfrac{\beta^2}{2\mathrm{Le}}\omega \\ \omega &= F\exp\big(\beta(\mathsf{T}-1)\big) \end{aligned} \tag{5}$$

arrived at from the model (1), with $D = \theta^2 Q^2/2\mathrm{Le}T_*^4 = \frac{1}{2}\beta^2/\mathrm{Le}$, by rescaling temperature such that $T \mapsto T_* + Q(\mathsf{T}-1)$, so that $T = T_*$ when $\mathsf{T} = 1$ (note the change in font), and by linearising the exponent in the reaction rate term about the rescaled temperature $\mathsf{T} = 1$, such that

$$\theta/T_* - \theta/T = \frac{\theta Q(\mathsf{T}-1)}{T_*^2\big(1+Q(\mathsf{T}-1)/T_*\big)} \sim \beta(\mathsf{T}-1) \quad \text{with} \quad \beta = \frac{\theta Q}{T_*^2}.$$

This defines the Zel′dovich number $\beta$, which is large because $\theta$ is large.

The only real change from the model (1), is the linearisation of the exponent in the reaction rate term. Equation (4) can be used to show that this makes no significant difference, to leading order, for changes in the flame temperature $\widehat{T}$ from the value $T_*$ that are of the order of $\theta^{-1}$. The jump conditions that arise using the full form of the Arrhenius exponent, in the absence of effects due to curvature, propagation and temperature gradients in the burnt gas, have already been found in equation (4) and can be brought back into account later on. The linearisation does, however, simplify the analysis of the chemistry for now. This will prove useful since we are about to introduce greater complexity by considering a more general geometry for the flame sheet in a more general flow field.

In particular, let us seek the asymptotic structure that a reaction region would have when the flame-sheet $\mathbf{\Gamma}$ is curved, when there is a non-uniform flow field and when temperatures in the reaction region are close to the value $\mathsf{T} = 1$. For simplicity, we can take the problem to be two dimensional, generalising the results to three dimensions later on, so that, at some moment in time $t$, the sheet can be taken to lie at $y = Y(t,x)$. By rotating coordinates at the time $t$ and shifting the origin to any point of interest, we can set $Y_x$ to be zero at $x = t = 0$. By allowing the reference frame to move, the flow field can

be described near $x = y = 0$ by setting $\mathbf{v} = \mathbf{0}$ at $x = y = 0$, with $\mathbf{v} = \big(\sigma_{\rm e}x + \sigma_{\rm s}y, -\sigma_{\rm e}y\big)$. If there is a constant and uniform rate of strain, then $\sigma_{\rm e}$ represents a diverging strain rate in the x-direction, converging in the y-direction, while $\sigma_{\rm s}$ represents a shear component of the vorticity after allowing the coordinate frame to rotate so as to remove any shear in the y-direction; such a component would serve to rotate the flame sheet and our choice of reference frame would then rotate with the sheet. More generally, $\sigma_{\rm e}$ and $\sigma_{\rm s}$ are of order one and may vary with space and time for order one values of $x$ and $y$, including any effects of thermal expansion that might be inherent in the model. However, for small values of $x$ and $y$ they may be taken to be constant to leading order.

If we now introduce the new variable $r$ to measure distances in the y direction ahead of the sheet, such that

$$r = y - Y(t, x)$$

then the equations (5) for $F$ and $\mathsf{T}$ can be transformed to the non-orthogonal reference frame of $(t, x, r)$, using

$$\begin{aligned}
\partial_y &\mapsto \partial_r, \quad \partial_x \mapsto \partial_x - Y_x\partial_r \\
\partial_{xx} + \partial_{yy} &\mapsto (1 + Y_x^2)\partial_{rr} - Y_{xx}\partial_r + \partial_{xx} - 2Y_x\partial_{rx} \\
\partial_t + (\mathbf{v}\cdot\nabla) &\mapsto \partial_t - Y_t\partial_r + \boldsymbol{v}\cdot(\partial_x, \partial_r) \\
\text{with} \quad \boldsymbol{v} &= \Big(\sigma_{\rm s}(Y{+}r){+}\sigma_{\rm e}x,\ -(\sigma_{\rm e}{+}\sigma_{\rm s}Y_x)(Y{+}r){-}\sigma_{\rm e}Y_x x\Big).
\end{aligned}$$

This gives

$$\begin{aligned}
\big(\partial_t - V\partial_r + \boldsymbol{v}\cdot(\partial_x, \partial_r)\big)F &= \big((1 + Y_x^2)\partial_{rr} - Y_{xx}\partial_r + \partial_{xx} - 2Y_x\partial_{rx}\big)\tfrac{1}{\rm Le}F - \tfrac{\beta^2}{2\rm Le}\omega \\
\big(\partial_t - V\partial_r + \boldsymbol{v}\cdot(\partial_x, \partial_r)\big)\mathsf{T} &= \big((1 + Y_x^2)\partial_{rr} - Y_{xx}\partial_r + \partial_{xx} - 2Y_x\partial_{rx}\big)\mathsf{T} + \tfrac{\beta^2}{2\rm Le}\omega
\end{aligned}$$

in which we have written $V = Y_t$ to denote the vertical speed of movement of the interface $y = Y(t, x)$, at any fixed value of $x$. At the point $x = 0$ where $Y_x = 0$ and $\mathbf{v} = \mathbf{0}$ at the time $t$, it represents the normal propagation speed of the interface relative to the medium. By eliminating $\omega$, we obtain the equation for the enthalpy

$$\big(\partial_t - V\partial_r + \boldsymbol{v}\cdot(\partial_x, \partial_r)\big)(\mathsf{T} + F) = \big((1 + Y_x^2)\partial_{rr} - Y_{xx}\partial_r + \partial_{xx} - 2Y_x\partial_{rx}\big)\big(\mathsf{T} + \tfrac{1}{\rm Le}F\big)$$

which shows that non-equidiffusive effects with $\rm Le \neq 1$ will tend to redistribute the dimensionless enthalpy, $h = \mathsf{T} + F$.

Broadly speaking, we can imagine that a thin reaction region forms part of a flame structure of some type, in which temperature and reactant concentration vary by order one over length and time scales (measured by $x$, $y$ and $t$) that are of order one. Thus the interface $y = Y(t, x)$ might have a curvature of order one and be moving at a speed $V = Y_t$ that is of order one. Because of the sensitive temperature dependence that has been identified for the jump in gradient across the reaction-sheet, which in turn should not change abruptly, the temperature at the sheet should not vary by more than the order of $\beta^{-1}$. To be consistent with this limitation, the temperature in the burnt gas (where values of $F$ must be transcendentally small) should also only vary by the order of $\beta^{-1}$ over length and time scales that are of order one.

Thus, without delving any more deeply into the nature of the burnt gas, where reactivity is transcendentally close to equilibrium ($F = 0$), we can simply assume the following

asymptotic nature of the burnt region near the flame sheet, when $r$ is small and negative

$$\mathsf{T} = \widehat{\mathsf{T}} + r\widehat{\mathsf{T}}_r + O(r^2\epsilon) \quad \text{and} \quad F = \overline{o}(\epsilon)$$
$$\text{with} \quad \widehat{\mathsf{T}}(t,x) = 1 + O(\epsilon) \quad \text{and} \quad \widehat{\mathsf{T}}_r(t,x) = O(\epsilon)$$

as $\epsilon \to 0$, with $\epsilon \ll -r \ll 1$. For the sake of more efficient notation, we have defined $\epsilon = \beta^{-1}$ and we use the symbol $\overline{o}(\cdot)$ to denote something that is transcendentally small. That is, $F = \overline{o}(\epsilon) \iff F = o(\epsilon^\nu)$, as $\epsilon \to 0$, for any power $\nu \in \mathbb{R}$. Thus we ensure that the temperature gradient is small in the burnt region, behind the reaction region, and that the temperature at the reaction sheet deviates only slightly from the temperature $\mathsf{T} = 1$. If we now rescale such that

$$F = \epsilon \mathrm{Le} f, \quad \mathsf{T} = 1 - \epsilon\phi, \quad r = \epsilon\eta$$

then, in order to match with the properties in the burnt region, the conditions that must be satisfied in the reaction region as $\eta \to -\infty$ are

$$\begin{gathered} \phi = \widehat{\phi} + \epsilon\eta\widehat{\phi}_r + O(\epsilon^2\eta^2) \quad \text{and} \quad f = \overline{o}(\epsilon) \\ \text{with} \quad \widehat{\mathsf{T}} = 1 - \epsilon\widehat{\phi} \quad \text{and} \quad \widehat{\mathsf{T}}_r = -\epsilon\widehat{\phi}_r \end{gathered} \tag{6}$$

as $\epsilon \to 0$. We can assume that $\widehat{\phi}(t,x)$ and $\widehat{\phi}_r(t,x)$ are both of order one as $\epsilon \to 0$.

The governing reactive diffusive equations describing the region of chemical reaction now become

$$(1+Y_x^2)f_{\eta\eta} - \tfrac{1}{2}f\mathsf{e}^{-\phi} + \epsilon(\mathrm{Le}V - Y_{xx})f_\eta = 2\epsilon Y_x f_{\eta x} + \mathrm{Le}\big(\epsilon^2 f_t + \boldsymbol{v}\cdot(\epsilon^2 f_x, \epsilon f_\eta)\big) - \epsilon^2 f_{xx}$$
$$(1+Y_x^2)\phi_{\eta\eta} - \tfrac{1}{2}f\mathsf{e}^{-\phi} + \epsilon(V - Y_{xx})\phi_\eta = 2\epsilon Y_x\phi_{\eta x} + \epsilon^2\phi_t + \boldsymbol{v}\cdot(\epsilon^2\phi_x, \epsilon\phi_\eta) - \epsilon^2\phi_{xx}$$

with

$$\boldsymbol{v} = \big(\sigma_\mathrm{s}(Y+\epsilon\eta) + \sigma_\mathrm{e}x, -(\sigma_\mathrm{e}+\sigma_\mathrm{s}Y_x)(Y+\epsilon\eta) - \sigma_\mathrm{e}Y_x x\big)$$

and, at the instant $t$, when coordinates have been chosen to set $Y_x(t,0) = 0$, we have

$$Y = \tfrac{1}{2}x^2 Y_{xx}(t,0) + O(x^3), \quad Y_x = xY_{xx}(t,0) + O(x^2).$$

Thus, taking $Y_{xx}$ to be of order one, and only considering values of $x$ that are of order $\epsilon$ (that is, considering only the region close to $x = 0$), we have that $\boldsymbol{v} = O(\epsilon)$. The convective terms containing $\boldsymbol{v}$ are then at most of order $\epsilon^2$.

Ignoring terms that are of order $\epsilon^2$ or smaller now gives

$$f_{\eta\eta} - \tfrac{1}{2}f\mathsf{e}^{-\phi} + \epsilon(\mathrm{Le}V - 2\kappa)f_\eta = O(\epsilon^2)$$
$$\phi_{\eta\eta} - \tfrac{1}{2}f\mathsf{e}^{-\phi} + \epsilon(V - 2\kappa)\phi_\eta = O(\epsilon^2)$$

in which we have used the expression for the mean curvature of the interface in three dimensions, $\kappa = Y_{xx}/2$ at $x = 0$, to write the equation in terms of the more generic parameter $\kappa$ rather than $Y_{xx}$. Both $V(t,x)$ and $\kappa(t,x)$ can be taken to be locally constant, changing very little on the small time and length scales that we are considering around the point $x = y = 0$ at the time $t$. Eliminating $\frac{1}{2}f\mathsf{e}^{-\phi}$ gives the enthalpy equation

$$\phi_{\eta\eta} - f_{\eta\eta} + \epsilon V(\phi_\eta - \mathrm{Le}f_\eta) - 2\epsilon\kappa(\phi_\eta - f_\eta) = O(\epsilon^2)$$

which can be solved iteratively, along with the matching conditions (6), to obtain the expression for $\phi$ in terms of $f$

$$\phi = \widehat{\phi} + f + \epsilon\eta\widehat{\phi}_r + \epsilon V(\mathrm{Le}-1)\int_{\widehat{\eta}}^{\eta} f\,\mathrm{d}\eta + O(\epsilon^2) \tag{7}$$

where $\eta = r/\epsilon = \widehat{\eta}(\epsilon) < 0$ is a position at which $f$ and $f_\eta$ are at most of order $\epsilon^2$. As will be seen later, we can find such positions with $\widehat{\eta} = -O(|\ln\epsilon|)$. The precise choice of $\widehat{\eta}$ is not important, provided $\epsilon\widehat{\eta} = o(1)$ as $\epsilon \to 0$.

Substituting for $\phi$ now gives

$$f_{\eta\eta} = \tfrac{1}{2} f e^{-\widehat{\phi}-f} + \epsilon V(1-\mathrm{Le}) f_{\eta\eta}\int_{\widehat{\eta}}^{\eta} f\,\mathrm{d}\eta - \epsilon\widehat{\phi}_r\,\eta f_{\eta\eta} + \epsilon(2\kappa - \mathrm{Le}V) f_\eta + O(\epsilon^2)$$

after using the leading order result, $f_{\eta\eta} = \frac{1}{2} f e^{-\widehat{\phi}-f} + O(\epsilon)$, to eliminate some occurences of $\frac{1}{2} f e^{-\widehat{\phi}-f}$. Multiplying by $2f_\eta$, integrating, by parts if necessary, and using the matching condition (6), now leads to the expression for $f_\eta$ in terms of $f$

$$\begin{aligned} f_\eta^2 = e^{-\widehat{\phi}}\Big(1-(1+f)e^{-f}\Big) + \epsilon V(1-\mathrm{Le})\bigg(f_\eta^2\int_0^f \frac{f}{f_\eta}\,\mathrm{d}f - \int_0^f f f_\eta\,\mathrm{d}f\bigg) \\ - \epsilon\widehat{\phi}_r\bigg(\eta f_\eta^2 - \int_0^f f_\eta\,\mathrm{d}f\bigg) + 2\epsilon(2\kappa - \mathrm{Le}V)\int_0^f f_\eta\,\mathrm{d}f + O(\epsilon^2). \end{aligned} \tag{8}$$

The sign of $f_\eta$ must be positive, so that $f_\eta = e^{-\widehat{\phi}/2}\sqrt{1-(1+f)e^{-f}} + O(\epsilon)$ to leading order. When $f$ is small, it follows that $f_\eta \sim f 2^{-1/2} e^{-\widehat{\phi}/2}$ and hence $f \sim \widehat{f}\exp\big(\eta\, 2^{-1/2} e^{-\widehat{\phi}/2}\big)$ for some suitable function $\widehat{f}(t,x)$. Solving for $\eta$, this demonstrates that $f = O(\epsilon^2)$ where $\eta = -2^{1/2} e^{\widehat{\phi}/2}|\ln\epsilon^2| + O(1)$, so that $\widehat{\eta}$ can be chosen such that $-\widehat{\eta} \geq 2^{5/2} e^{\widehat{\phi}/2}|\ln\epsilon| + O(\epsilon)$.

Also since $f_\eta \sim e^{-\widehat{\phi}/2}\sqrt{1-(1+f)e^{-f}}$, the integrals in the expression (8) can be reformulated as follows

$$\begin{aligned} \int_0^f f_\eta\,\mathrm{d}f &= e^{-\widehat{\phi}/2}\int_0^f \sqrt{1-(1+\tau)e^{-\tau}}\,\mathrm{d}\tau \;+\; O(\epsilon) \;\;\sim\; e^{-\widehat{\phi}/2}\Big(f - \varpi\Big) \\ \int_0^f f f_\eta\,\mathrm{d}f &= e^{-\widehat{\phi}/2}\int_0^f \tau\sqrt{1-(1+\tau)e^{-\tau}}\,\mathrm{d}\tau + O(\epsilon) \;\sim\; e^{-\widehat{\phi}/2}\Big(\tfrac{1}{2}f^2 - \varpi_1\Big) \\ \int_0^f \frac{f}{f_\eta}\,\mathrm{d}f &= e^{\widehat{\phi}/2}\int_0^f \frac{\tau}{\sqrt{1-(1+\tau)e^{-\tau}}}\,\mathrm{d}\tau \;+\; O(\epsilon) \;\sim\; e^{\widehat{\phi}/2}\Big(\tfrac{1}{2}f^2 + \varpi_2\Big). \end{aligned} \tag{9}$$

Unfortunately, none of these integrals can be evaluated in terms of elementary functions, but they do each approach the asymptotic forms shown on the right exponentially quickly as $f$ becomes large. Noting that

$$\begin{aligned} \varpi_1 + \varpi_2 &= \int_0^\infty \tau\Big(1-\sqrt{1-(1+\tau)e^{-\tau}}\Big)\mathrm{d}\tau + \int_0^\infty \Big(\frac{\tau}{\sqrt{1-(1+\tau)e^{-\tau}}} - \tau\Big)\mathrm{d}\tau \\ &= 2\int_0^\infty (1+\tau)\frac{\frac{1}{2}\tau e^{-\tau}}{\sqrt{1-(1+\tau)e^{-\tau}}}\,\mathrm{d}\tau \\ &= 2\Big[(1+f)\sqrt{1-(1+f)e^{-f}} - \int_0^f \sqrt{1-(1+\tau)e^{-\tau}}\,\mathrm{d}\tau\Big]_0^\infty \\ &= 2(1+\varpi) \end{aligned}$$

the constants given in these formulae are seen to be related by $1+\varpi=\frac{1}{2}(\varpi_1+\varpi_2)$.

Hence, although the formula (8) cannot be evaluated easily beyond its leading-order, it does approach the simple asymptotic behaviour for large values of $f$ or $\eta$:

$$f_\eta = \mathsf{e}^{-\widehat{\phi}/2} + \epsilon V(1-\mathrm{Le})(1+\varpi) - \tfrac{1}{2}\epsilon\widehat{\phi}_r\mathsf{e}^{-\widehat{\phi}/2}\,\eta \\ + \epsilon\big(\tfrac{1}{2}\widehat{\phi}_r + 2\kappa - \mathrm{Le}V\big)(f-\varpi) + O(\epsilon^2,\mathsf{e}^{-f}).$$

Thus, while the formula (8) matches with properties expected in the burnt region for large negative values of $\eta$, where $f\to 0$, it is also linked with the region of "preheating," where $f\gg 1$, through this asymptotic result for large positive values of $\eta$ and $f$. Moreover, because the asymptote is approached exponentially quickly as $f$ grows, it can be integrated, iteratively, to provide the asymptotic behaviour of $f$ at large $\eta$:

$$f = \Big(\mathsf{e}^{-\widehat{\phi}/2} + \epsilon V(1-\mathrm{Le})(1+\varpi) \\ - \epsilon\big(\tfrac{1}{2}\widehat{\phi}_r + 2\kappa - \mathrm{Le}V\big)\varpi\Big)\Big(\eta + \epsilon(2\kappa-\mathrm{Le}V)\tfrac{1}{2}\eta^2\Big) + O(\epsilon^2,\mathsf{e}^{-\phi}).$$

In arriving at this result, a function of integration has been chosen such that $f\to 0$ as $\eta\to 0^+$. This amounts to defining the location of the path $y=Y(t,x)$, or $\eta=r=0$, such that the extrapolation of this *asymptotic form* for $f$ at large values of $\eta$, back to $\eta=0^+$, gives the value zero for $f$. Equation (7) now takes on the asymptotic form for large $\eta$

$$\phi = \widehat{\phi} + f + \epsilon\widehat{\phi}_r\eta + \epsilon V(\mathrm{Le}-1)\mathsf{e}^{-\widehat{\phi}/2}\tfrac{1}{2}\eta^2 + O(\epsilon^2,\mathsf{e}^{-\phi}).$$

These equations now provide the necessary far-field asymptotic behaviour of the solution in the reaction region for matching with a region of "preheating" where $F>0$ and $f\gg 1$.

The matching requirement that arises for $F(t,x,r)$ and $\mathsf{T}(t,x,r)$, in this preheating region as $r\to 0^+$, therefore takes on the form

$$\frac{F}{\mathrm{Le}} = \widehat{\mathsf{T}} - \mathsf{T} + r\widehat{\mathsf{T}}_r + \tfrac{1}{2}r^2(1-\mathrm{Le})V\mathsf{e}^{(\widehat{\mathsf{T}}-1)/2\epsilon} + O(\epsilon^2,r^3) \\ = \Big(\mathsf{e}^{(\widehat{\mathsf{T}}-1)/2\epsilon} + \epsilon\big(1+\varpi-\mathrm{Le}\big)V + \big(\tfrac{1}{2}\widehat{\mathsf{T}}_r - 2\epsilon\kappa\big)\varpi\Big)\big(r - \tfrac{1}{2}r^2(\mathrm{Le}V-2\kappa)\big) + O(\epsilon^2,r^3).$$

Alternatively, the requirement for matching of the derivatives $F_r$ and $\mathsf{T}_r$ is

$$\tfrac{1}{\mathrm{Le}}F_r = \Big(\mathsf{e}^{(\widehat{\mathsf{T}}-1)/2\epsilon} + \epsilon\big(1+\varpi-\mathrm{Le}\big)V + \big(\tfrac{1}{2}\widehat{\mathsf{T}}_r - 2\epsilon\kappa\big)\varpi\Big)\big(1-r(\mathrm{Le}V-2\kappa)\big) + O(\epsilon^2,r^2)$$

$$\widehat{\mathsf{T}}_r - \mathsf{T}_r = \Big(\mathsf{e}^{(\widehat{\mathsf{T}}-1)/2\epsilon} + \epsilon\big(1+\varpi-\mathrm{Le}\big)V + \big(\tfrac{1}{2}\widehat{\mathsf{T}}_r - 2\epsilon\kappa\big)\varpi\Big)\big(1-r(V-2\kappa)\big) + O(\epsilon^2,r^2).$$

Evaluated as $r\to 0^+$, these equations provide the jumps in the values of the gradients of $F$ and $\mathsf{T}$ across an apparent flame sheet at $r=0$, accurate to order $\epsilon$, as $\epsilon\to 0$.

We have therefore shown that a more complete form of the gradient jump conditions, that arises at a flame sheet for the model (5), is

$$\tfrac{1}{\mathrm{Le}}[F_n] = -[\mathsf{T}_n] = \mathsf{e}^{\beta(\mathsf{T}-1)/2} + \big(1+\varpi-\mathrm{Le}\big)V/\beta + \varpi\big(\tfrac{1}{2}\mathsf{T}_n^- - 2\kappa/\beta\big) + O(\beta^{-2}) \qquad (10)$$

as $\beta\to\infty$, where $V$ is the normal propagation speed of the sheet relative to the medium, $\kappa$ is the mean curvature of the sheet and $\mathsf{T}_n^-$ is the normal gradient of temperature on the burnt side, expected to be of the order of $\beta^{-1}$ in value. Any strain rate and shear rate in the flow, that change the fluid velocity by order one over lengths that are of the order of the thickness of the preheating region, can only affect the jump conditions at the flame sheet by an amount of the order of $\beta^{-2}$. Unsteadiness and transverse diffusion along the flame sheet also affect the jump conditions at or below this order of magnitude.

## 3.3 High-order flame sheet model

More generally, in terms of the dimensionless absolute temperature $T$ of equations (1) or (2), for which we now rescale $\mathsf{T} \mapsto 1 + (T - T_*)/Q$, thus inverting the scaling that defined $\mathsf{T}$, with the Damköhler number set to $D = \delta^2 \frac{1}{2}\beta^2/\mathrm{Le}$, which amounts to rescaling $t \mapsto \delta^2 t'$, $\mathbf{x} \mapsto \delta \mathbf{x}'$ and $\mathbf{v} \mapsto \mathbf{v}'/\delta$, we have, after dropping the primes and using the result (4) to compensate for the linearisation of the Arrhenius exponent in (5)

$$\left.\begin{aligned} F_t + \mathbf{v}\cdot\nabla F &= \tfrac{1}{\mathrm{Le}}\nabla^2 F \\ T_t + \mathbf{v}\cdot\nabla T &= \nabla^2 T \end{aligned}\right\} \quad \text{for} \quad \mathbf{x} \notin \mathbf{\Gamma}$$

$$\left.\begin{aligned} [T] = [F] = F &= 0 \\ \tfrac{1}{\mathrm{Le}}[F_n] = -\tfrac{1}{Q}[T_n] &= \Omega \end{aligned}\right\} \quad \text{at} \quad \mathbf{x} \in \mathbf{\Gamma} \tag{11}$$

$$\text{with} \quad \Omega = \delta \tfrac{T^2}{T_*^2} \exp\left(\tfrac{\theta}{2}\tfrac{T-T_*}{TT_*} - 3\tfrac{T}{\theta}\right) + \tfrac{1+\varpi-\mathrm{Le}}{Q} V \tfrac{T^2}{\theta} + \tfrac{\varpi}{Q}\left(\tfrac{1}{2}T_n^- - 2\kappa\tfrac{T^2}{\theta}\right) + O(\theta^{-2})$$

in which the propagation speed of the sheet relative to the flow is $V = (\partial_t \mathbf{\Gamma} - \mathbf{v})\cdot\widehat{\mathbf{n}}$, where $\widehat{\mathbf{n}}$ is a unit normal to $\mathbf{\Gamma}$ pointing towards increasing values of the reactant $F$. The constant $\varpi$ is defined by an asymptotic relation in equations (9) for large $f$, having the integral expression and numerical value

$$\varpi = \int_0^\infty \left(1 - \sqrt{1 - (1+\tau)e^{-\tau}}\right) \mathrm{d}\tau = 1.34404568\cdots$$

when calculated to nine significant figures.

The most significant generalisation in this model from the model (2) is not the addition of terms that depend weakly on temperature, since these are dominated by the sensitivity of the chemistry to small changes in temperature at leading order, but the appearance of a relatively weak dependence of the jump conditions on propagation speed $V$, mean curvature $\kappa$ and conduction into the burnt gas via $T_n^-$. Increasing the normal propagation speed $V$ increases the jump in gradients, for Lewis numbers $\mathrm{Le} < 1 + \varpi$, and increasing the mean curvature $\kappa$ decreases the jump in gradients. A weak conductive heat loss into the medium behind the flame, for which $T_n^- > 0$, also causes a weak increase in the jump in gradients. These are all weak effects, being of the order of $\theta^{-1}$. Increasing the temperature $T$ at the flame sheet has a considerably stronger effect. Temperature changes would typically have to be very small, of the order of $\theta^{-2}$, in order for these additional dependences to have an effect that is similar in magnitude to the effect of temperature.

In most practical situations therefore, when the activation temperature is large enough, this extension of the flame-sheet conditions to higher orders is unlikely to do more than add minor corrections to the simpler leading order model. There may be circumstances however where temperature changes are genuinely small and thus the higher order effects may by relevant to leading order.

## 3.4 Order one temperature gradients

The jump conditions in (10) and (11) are valid for small temperature gradients $T_n^-$ in the burnt gas, taken to be of the order of $\theta^{-1}$ in the derivation given above. However, while the

dimensionless mean curvature $\kappa$ and the propagation speed $V$ are unlikely ever to become large, there may be circumstances in which $T_n^-$ is not small, as may arise in partially premixed flames or flame balls surrounding sources of heat (see for example [8, 9]).

The matching conditions (6) can then be considered to have the form

$$\phi = \widehat{\phi} - \eta \mathsf{T}_n^- + O(\epsilon\eta^2) \quad \text{and} \quad f\mathrm{e}^{-\phi} = \overline{o}(\epsilon)$$

as $\epsilon \to 0$, with $1 \ll -\eta \ll \epsilon^{-1/2}$, in which we assume that $\mathsf{T}_n^-$ is of order one as $\epsilon \to 0$. The condition that $f\mathrm{e}^{-\phi} = \overline{o}(\epsilon)$ amounts to the condition on $f$ in (6) when $\phi = O(1)$, but when $\mathsf{T}_n^-$ is order one and positive, the condition can also be satisfied with $f \neq \overline{o}(\epsilon)$ since we then find that $\mathrm{e}^{-\phi} = \overline{o}(\epsilon)$ as $\epsilon \to 0$, with $1 \ll -\eta \ll \epsilon^{-1/2}$. As will be discussed shortly, a suitable condition for $f$ in the "burnt" gases then becomes

$$f = \begin{cases} \widehat{f} + \eta f_\eta^- + O(\epsilon\eta^2) & \text{for } \mathsf{T}_n^- > 0 \\ \overline{o}(\epsilon) & \text{for } \mathsf{T}_n^- \leq 0. \end{cases} \tag{12}$$

We can think of the constants $\widehat{f}$ and $f_\eta^-$ as both being necessarily zero when $\mathsf{T}_n^- \leq 0$. Otherwise, the value of $f_\eta^-$ must be either zero or negative to ensure that $f$ remains positive at large negative values of $\eta$. The flame-sheet, extrapolated from the solution when $\eta$ is large, is anticipated to be normalised to fall at $\eta = 0$, as before; this amounts simply to defining the origin of $\eta$. Thus, where the asymptotic solutions for large positive and large negative values of $\eta$ intersect (at $\eta = 0$), the extrapolated values of $f$ and $\phi$ become $\widehat{f}$ and $\widehat{\phi}$, respectively.

For simplicity, as was done in section 3.1, we can adopt a model in which all extraneous effects are removed. Let us therefore consider $\partial_t = \partial_x = \boldsymbol{v} = V = \kappa = 0$, with $f = f(\eta)$ and $\phi = \phi(\eta)$, satisfying the equations

$$\phi_{\eta\eta} = f_{\eta\eta} = \tfrac{1}{2} f\mathrm{e}^{-\phi}$$

and matching conditions

$$\phi \sim \widehat{\phi} - \eta \mathsf{T}_n^-, \quad f \sim \widehat{f} + \eta f_\eta^-$$

as $\eta \to -\infty$, immediately revealing that

$$\phi = f + \widehat{\phi} - \widehat{f} - \eta(\mathsf{T}_n^- + f_\eta^-), \quad f_{\eta\eta} = \tfrac{1}{2}\mathrm{e}^{\widehat{f}-\widehat{\phi}} f \mathrm{e}^{\eta(\mathsf{T}_n^- + f_\eta^-) - f}.$$

It is more convenient, however, to examine the related problem

$$f_{\zeta\zeta} = \tfrac{1}{2} f\mathrm{e}^{\alpha\zeta - f}, \quad f \sim \begin{cases} \widehat{f} + \left(\zeta - \widehat{\zeta}\right) f_\zeta^- & \text{as } \zeta \to -\infty \\ \widehat{f} + \left(\zeta - \widehat{\zeta}\right) f_\zeta^+ & \text{as } \zeta \to +\infty \end{cases} \tag{13}$$

in which both forms of asymptotic behaviour, at large positive and large negative values of $\zeta$, are now taken to extrapolate to an intersection at $\zeta = \widehat{\zeta}$. By defining

$$\eta = \left(\zeta - \widehat{\zeta}\right) \mathrm{e}^{(\alpha\widehat{\zeta} + \widehat{\phi} - \widehat{f})/2}, \quad f_\eta^\pm = f_\zeta^\pm \mathrm{e}^{(\widehat{f} - \widehat{\phi} - \alpha\widehat{\zeta})/2}, \quad \mathsf{T}_n^- + f_\eta^- = \alpha \mathrm{e}^{(\widehat{f} - \widehat{\phi} - \alpha\widehat{\zeta})/2} \tag{14}$$

the solution in terms of $\eta$ is reproduced and the extrapolated solutions at infinity intersect at $\eta = 0$, as required. We can now see that, if $\alpha > 0$, which is only possible if $\mathsf{T}_n^- > 0$, then $f_{\zeta\zeta}$ can become exponentially small at large negative values of $\zeta$, or $\eta$, without $f$

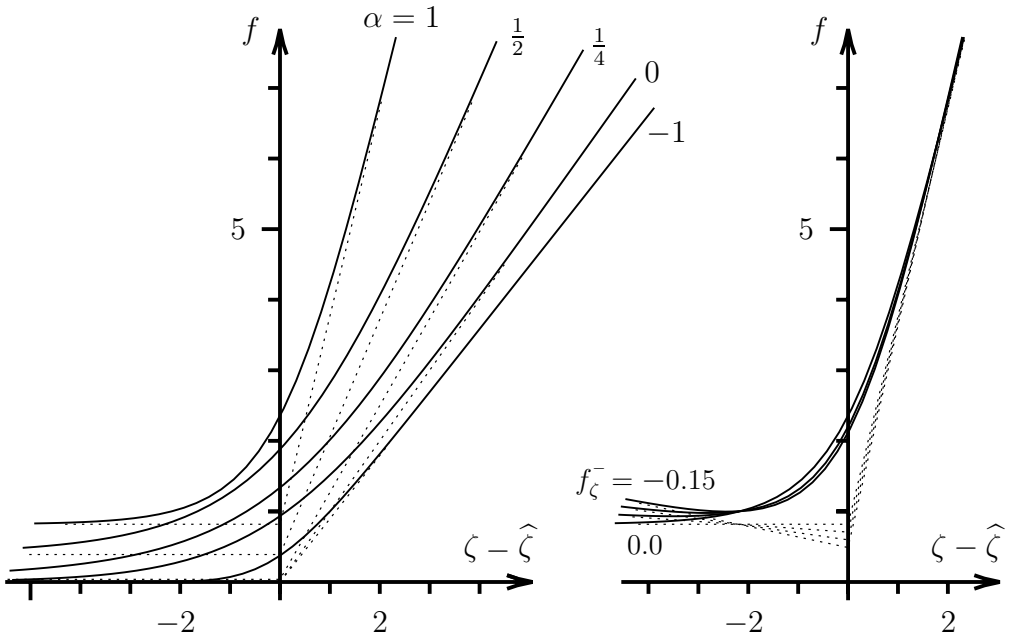


Figure 1: Variation of $f$ with $\zeta$ for different values of $\alpha$, having $f_\zeta^- = 0$ (left), and for different values of $f_\zeta^-$, having $\alpha = 1$ (right). For clarity of presentation the curves are all shifted so that the asymptotes intersect at the origin; the point where $f = 1$ then determines the value of $\widehat{\zeta}$.

itself being exponentially small. For this reason, the asymptotically linear behaviour of $f$, already introduced in equation (12), becomes possible when $\mathsf{T}_n^- > 0$.

When $\alpha = 0$, the work in section 3.2 makes clear that $f_\zeta \to 1$ as $\zeta \to \infty$. Also, when $\alpha$ is small, it shows that $f_\zeta \to 1 + \frac{1}{2}\varpi\alpha$. Increasing $\alpha$ thus tends to increase the change in $f_\zeta$, and hence $F_n$, across the reaction sheet. As $\alpha$ becomes larger, the effect grows; positive values of $\alpha$ enhance the reaction-rate in equations (13), when $\zeta$ is positive, and $f$ is growing.

Equations (13) were solved using a shooting method. Conveniently, the value $f = 1$ (or any other constant value) can now be adopted at $\zeta = 0$, without loss of generality. Given suitable values of $\alpha$ and $f_\zeta^- \le 0$, a value of $f_\zeta$ was chosen at $\zeta = 0$ and used to shoot towards negative values of $\zeta$ until either $f$ became negative or $f_{\zeta\zeta}$ became negligibly small. The value of $f_\zeta$ was then varied at $\zeta = 0$ so as to find a solution having $f > 0$, with $f_{\zeta\zeta} \to 0$ and $f_\zeta \to f_\zeta^-$ as $\zeta \to -\infty$. The same values of $f$ and $f_\zeta$, at $\zeta = 0$, were then used to shoot towards large enough positive values of $\zeta$ for $f_{\zeta\zeta}$ to become negligibly small again, providing the value of $f_\zeta^+$, as the limiting value of $f_\zeta$ as $\zeta \to \infty$. Both linear forms of behaviour (for $\zeta \gg 1$ and $-\zeta \gg 1$) were then extrapolated to find their point of intersection, at $(f, \zeta) = \big(\widehat{f}, \widehat{\zeta}\big)$. The transformation (14) then provided the corresponding solution in terms of $\eta$.

Some results are shown in Figure 1, where $f$ is plotted as a function of $\zeta - \widehat{\zeta}$ (for clarity of presentation). The effects of varying both $\alpha$ and $f_\zeta^-$ (when $\alpha > 0$) are shown. As well as increasing the value of $f_\zeta^+$, increasing $\alpha$ also increases the value of $\widehat{f}$, above zero, when $\alpha > 0$. At a fixed positive value of $\alpha$, decreasing $f_\zeta^-$, below zero, decreases the value of $\widehat{f}$.

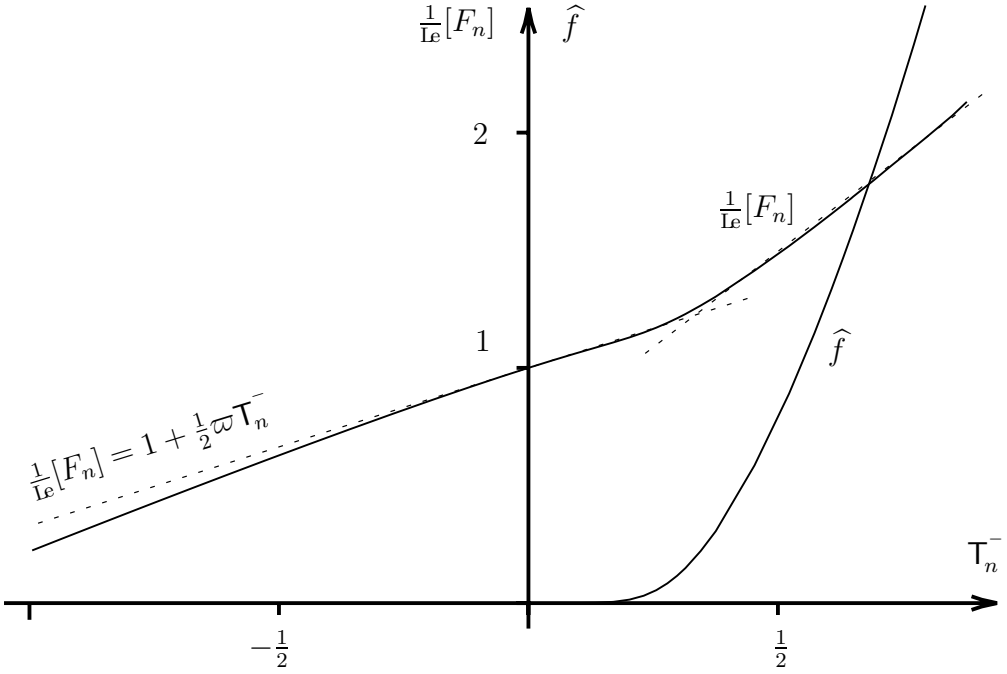


Figure 2: Dependence of the jump in reactant gradient, $\frac{1}{\mathrm{Le}}[F_n]$, and fuel leakage $\widehat{f}$, on order one variations in the temperature gradient $\mathsf{T}_n^-$ in the burnt gases, when $f_\eta^- = 0$ and the flame-sheet temperature is exactly unity. The dotted lines are the path on which $\frac{1}{\mathrm{Le}}[F_n] = 1 + \frac{1}{2}\varpi \mathsf{T}_n^-$ and the line $\frac{1}{\mathrm{Le}}[F_n] = 0.68 + 1.63 \times \mathsf{T}_n^-$.

Considering only cases in which $f_\zeta^- = 0$, which is the most natural condition for flames, Figure 2 provides the resulting jump in the value of $F_n$, or $f_\eta$, across the flame sheet, as a function of the temperature gradient $\mathsf{T}_n^-$ in the burnt gas. The jump is found to remain remarkably close to its limiting form, $\frac{1}{\mathrm{Le}}[F_n] = 1 + \frac{1}{2}\varpi \mathsf{T}_n^-$, for small values of $\mathsf{T}_n^-$, shown by the dotted line, over a significant range of values of $\mathsf{T}_n^-$. It deviates for $\mathsf{T}_n^- > \frac{1}{4}$ when the amount of fuel that leaks through the flame sheet, $F = \epsilon \mathrm{Le} \widehat{f}$, begins to grow significantly. In this range, the value of $[F_n]$ is closely approximated by another straight line, so that a reasonable approximation to the dependence of the flame-sheet jump conditions on $\mathsf{T}_n^-$ is given by

$$\frac{1}{\mathrm{Le}}[F_n] = -[\mathsf{T}_n] = e^{\beta(\mathsf{T}-1)/2} + \max\left\{1 + \tfrac{1}{2}\varpi \mathsf{T}_n^-,\ 0.68 + 1.63 \times \mathsf{T}_n^-\right\}$$

over the range $-1 < \mathsf{T}_n^- < 1$. The numerical solution of equations (13) thus shows that the linear dependence identified earlier, of the jump conditions on $\mathsf{T}_n^-$, remains reasonably good for values of $\mathsf{T}_n^-$ less than about one quarter.

# 4 Finite activation temperature

In situations where the dimensionless activation temperature is fixed in value, even though it may be reasonably large, equation (11) provides a means of estimating the errors that would arise through adopting only the leading order temperature dependence of the jump conditions at a flame sheet.

A useful example, to illustrate this, arises in considering a model for non-adiabatic, spherically symmetric flame balls, as studied in [5]–[7]. In [7], numerical solutions, found using an Arrhenius chemical model were compared with asymptotic solutions based on the corresponding leading order jump conditions. It was found that inordinately large Zel′dovich numbers, of the order of $\beta = 100$, were needed to obtain reasonably good comparisons. It is generally thought that realisitc values of the Zel′dovich number are of the order of ten or twenty, and that these are adequate to justify the use of leading order asymptotics. The numerical comparisons in [7] indicate that this assumption may be far from adequate for non-adiabatic flame balls. It would appear that higher order effects played a major role in these calculations for moderate values of $\beta$.

If we adopt the scaling for temperature $T \mapsto 1 + \frac{Q}{\mathrm{Le}}\mathsf{T}$ (note the font), set $T_* = 1 + \frac{Q}{\mathrm{Le}}$ and select $\delta = \frac{1}{\mathrm{Le}}$, the model takes the form

$$\begin{gathered}
\mathrm{Le} F_t = F_{rr} + \tfrac{2}{r}F_r \quad \text{and} \quad \mathsf{T}_t = \mathsf{T}_{rr} + \tfrac{2}{r}\mathsf{T}_r - \beta^{-1} b\, H(R-r) \quad \text{for} \quad r \neq R \\
\text{with} \quad |F| < \infty, \quad |\mathsf{T}| < \infty, \quad \lim_{r\to\infty} F = 1, \quad \lim_{r\to\infty} \mathsf{T} = 0 \quad \text{and} \\
[\mathsf{T}] = [F] = F = 0, \quad [F_r] = -[\mathsf{T}_r] = \Omega \quad \text{at} \quad r = R^{\pm}, \\
\Omega = \mathsf{e}^{\frac{1}{2}\beta(\mathsf{T}-1)} + (1 + \varpi - \mathrm{Le})\, R_t/\beta + \tfrac{1}{2}\varpi\, \mathsf{T}_r^{-} + 2\beta^{-1}\,\varpi/R
\end{gathered} \tag{15}$$

in which the Zel′dovich number is $\beta = Q\theta/\mathrm{Le}T_*^2 \gg 1$ and $r$ now represents a radial coordinate in a spherically symmetric structure, taking $F = F(t,r)$ and $\mathsf{T} = \mathsf{T}(t,r)$, with $r \geq 0$. A reaction sheet is taken to exist at the spherical surface, $r = R(t)$, leading to the jump conditions shown in (15), in which it is simplest, and sufficient to illustrate the importance of higher order terms, to consider only the linearised Arrhenius exponent as obtained in (10). For a sphere the mean curvature is $\kappa = -1/R$.

The problem is non-adiabatic because the parameter $b$ represents a constant heat-loss. The Heaviside function $H(R-r)$ ensures that it operates only in the burnt gases [5]–[7], where $r < R$. Taking $F$ and $\mathsf{T}$ to be bounded ensures that there is no source of reactant or heat at the origin, while the conditions at infinity fix the nondimensionalisation such that $T(t,\infty) = 1$, with $F$ also scaled against the value found for the reactant mass-fraction at large distances from the flame ball.

Details of the model and its physical origins can be found in [5]–[7] where it is studied in the asymptotic limit $\beta \to \infty$, using only the leading order term $\Omega = \mathsf{e}^{\frac{1}{2}\beta(\mathsf{T}-1)}$ for the jump conditions at the flame sheet. The equivalent problem, in which an Arrhenius rate law is used to model the chemistry, instead of jump conditions, is arrived at by adding $\frac{1}{2}\beta^2\omega$ to the right hand side of the equation for temperature $\mathsf{T}$ and subtracting $\frac{1}{2}\beta^2\omega$ from the equation for reactant $F$, taking $\omega = F\mathsf{e}^{\beta(\mathsf{T}-1)}$ as in equations (5). Details of the numerical solution of the latter form of the problem as well as the solution of the problem using jump conditions are described in [7].

Steady flame balls, for which $\partial_t \equiv 0$, are described by the solution

$$F = \begin{cases} 1 - R/r & : r \geq R \\ 0 & : r \leq R \end{cases} \quad \text{and} \quad \mathsf{T} = \begin{cases} \widehat{\mathsf{T}}R/r & : r \geq R \\ \widehat{\mathsf{T}} + \frac{1}{6}b(r^2 - R^2)/\beta & : r \leq R. \end{cases}$$

The condition $[F_r] = -[\mathsf{T}_r]$ provides an expression for the temperature at the flame sheet, $\widehat{\mathsf{T}} = 1 - \frac{1}{3}bR^2/\beta$, using which the condition $[F_r] = \Omega$ provides an expression relating the

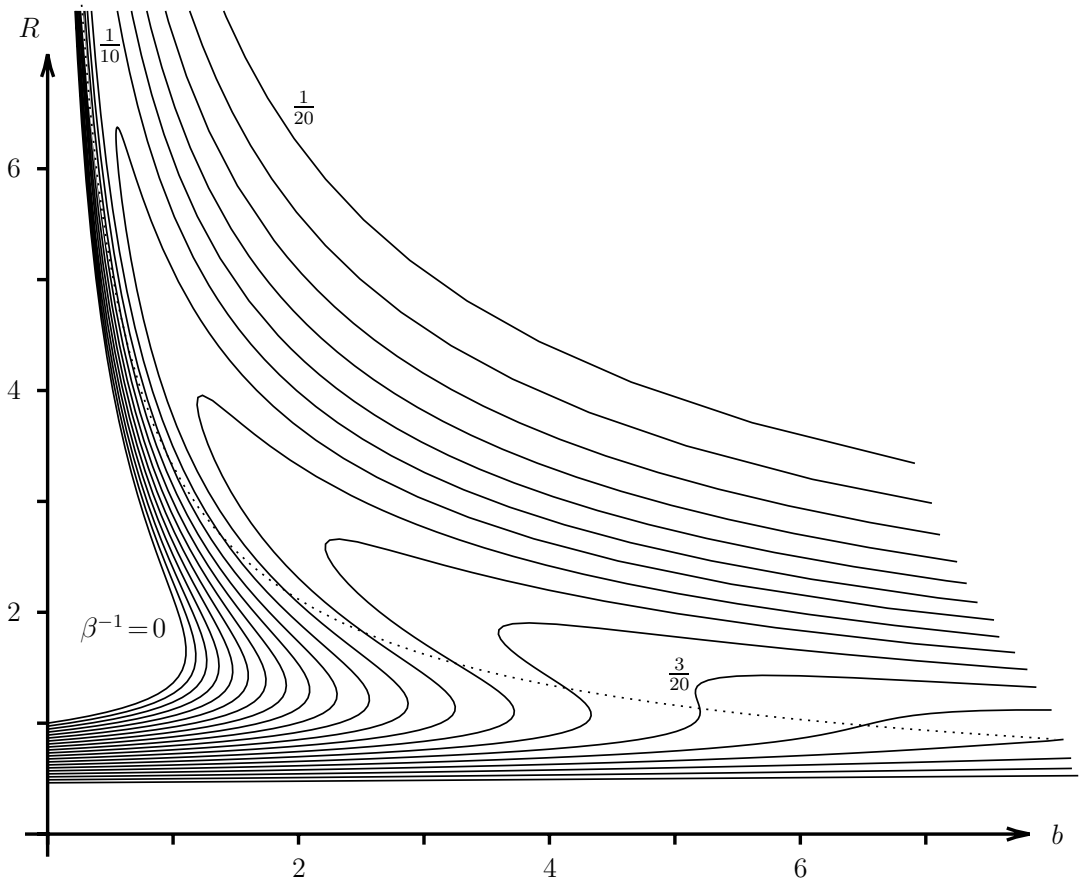


Figure 3: Variation of steady flame-ball radii $R$ with heat loss $b$ at various Zel′dovich numbers $\beta$, according to the higher-order asymptotic formula (16). The dotted curve marks the path on which $bR^2 = \beta$.

steady radius $R$ and the heat-loss parameter $b$, namely $R\mathrm{e}^{-bR^2/6} = 1 - \frac{\varpi}{\beta}(2 + \frac{1}{6}bR^2)$, or

$$R = \big(1 - \tfrac{\varpi}{\beta}(2+s)\big)\mathrm{e}^s, \quad b = 6s/R^2 \tag{16}$$

when parameterised in terms of $s = bR^2/6$. Curves relating $R$ and $b$ for various values of $\beta$ are presented in Figure 3.

If no account had been taken of the higher order terms, this would have given $R = \mathrm{e}^{bR^2/6}$, the same value as would have been found in the limit as $\beta \to \infty$. As described by the dashed curve in Figure 4, this provides a value of $R = 1$ when $b = 0$, with values of $R$ increasing with $b$ until a turning point is reached at $(b, R) = (3/\mathrm{e}, \mathrm{e}^{1/2})$, after which $R$ increases without bound as $b$ decreases towards zero.

For large but finite values of $\beta$, the deviation of the flame-ball radius $R$ from this behaviour as $\beta \to \infty$ becomes of order one when $bR^2 = O(\beta)$. The branch of solutions for which $R$ is large is therefore particularly affected by the higher order terms. In fact, as seen in Figure 3, the formula (16) provides a second turning point, for large enough values of $\beta$, after which values of $b$ increase again and $R$, ultimately, decreases as $b$ increases. For large enough values of $\beta$, there are therefore three solutions over some interval of values of the heat loss parameter $b$. For values of $\beta$ below about six, the two turning points merge and there is then only one value of $R$ for any value of $b$.

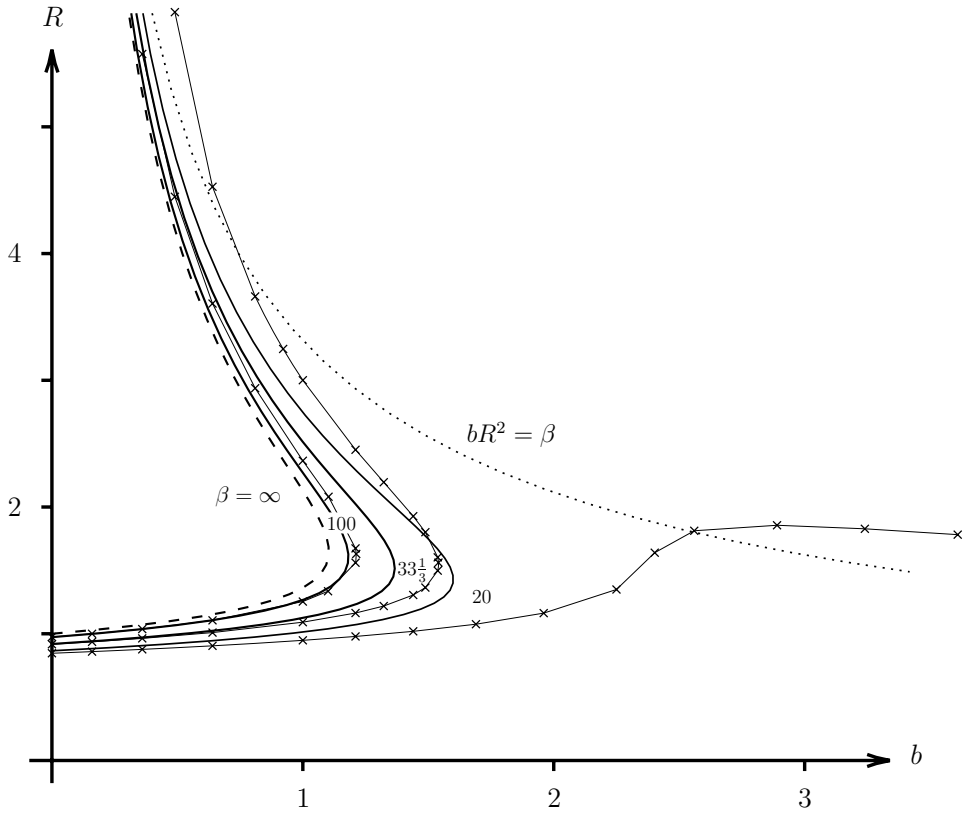


Figure 4: Variation with the heat loss parameter $b$ of numerically calculated steady flame-ball radii $R$, using Arrhenius kinetics to model the chemistry, at the Zel′dovich numbers $\beta = 100$, $33\frac{1}{3}$ and 20 (shown by the crosses, $\times$ ). The dashed curve and the full curves show the variation predicted by the higher-order asymptotic formula (16). The dotted curve marks the path on which $bR^2 = \beta$.

Of course, the equation (16) is not valid when $bR^2 = O(\beta)$, and the higher-order behaviour seen in Figure 3 cannot then be expected to be predicted accurately. The dotted line in the figure corresponds to the path where $bR^2 = \beta$ and for larger values of $R$ and $b$ significant differences are likely to arise between an accurate numerical simulation and the higher-order asymptotic prediction (16). Relevant numerical solutions are shown in Figure 4 for values of $\beta$ of 100, $33\frac{1}{3}$ and 20. The numerical results at $\beta = 33\frac{1}{3}$ can be seen to already deviate significantly from the higher-order asymptotic result at larger values of $R$, while the results at $\beta = 20$ deviate so much that the turning point is already lost. These large differences all appear where $bR^2 \geq O(\beta)$ and the higher-order asymptotic solutions cannot be expected to be accurate.

This example is most significant in showing that qualitatively and quantitatively important deviations from solutions based on the usual leading order description of jump conditions at a flame sheet can arise even for relatively large values of the Zel′dovich number, in this case for $\beta$ less than about thirty. Physically realistic values of about ten, which are often thought to be adequate because of the exponential sensitivity of reaction-rates to changes in temperature, are simply far too low for the leading order asymptotic description to apply.

Descriptions of other types of flames may also find that higher-order effects become

of overwhelming importance at realistic Zel′dovich numbers.

# 5 Conclusions

The higher-order jump conditions (11) provide a generalisation from the usual leading order jump conditions assumed at a reaction-sheet in combustion theory. They provide at least one means of testing the validity of leading order solutions and of predicting where they are likely to fail. In the case of flame balls with constant heat loss in the burnt gases [5]–[7], leading order asymptotic results fail quite dramatically for Zel′dovich numbers that are still moderately large, indeed realistic in value.

This raises some interesting and fundamental questions about the modelling of premixed flames and the current state of the art in describing flame balls and other types of laminar flame, using one-step chemistry. The formula (11) provides one means of testing and addressing these questions.

**Acknowledgements:** The authors are grateful to the EPSRC for financial support and to the IMA in Minneapolis for academic and computing support, as well as hospitality.

# References

[1] J.D. Buckmaster, G.S.S. Ludford (1982). Theory of Laminar Flames. Cambridge University Press.

[2] Ya.B. Zeldovich, G.I. Barrenblatt, V.B. Librovich, G.M. Makhviladze (1985). The Mathematical Theory of Combustion and Explosions. Consultants Bureau, New York.

[3] F.A. Williams (1985). Combustion Theory. Benjamin/Cummings, California.

[4] Sivashinsky, G.I. (1983). Instabilities, pattern formation and turbulence in flames. Annual Rewiews of Fluid Mechanics 15. 179–199.

[5] Buckmaster, J.D., Joulin, G., Ronney, P. (1990). The structure and stability of Nonadiabatic flame balls. Combustion and Flame 79. 381–392.

[6] Buckmaster, Joulin, Ronney Buckmaster, J.D., Joulin, G., Ronney, P. (1991). The structure and stability of Nonadiabatic flame balls: The effects of far-field losses. Combustion and Flame 84. 411–422.

[7] Shah, A.A., Thatcher, R.W., Dold, J.W. (2000). Stability of a spherical flame ball in a porous medium. Combustion Theory and Modelling 4. 511–534.

[8] N. Peters (2000). Turbulent Combustion. Cambridge University Press.

[9] Joulin, G. (1985). Point source initiation of lean spherical flames of light reactants: an asymptotic study. Combustion Science and Technology 43. 99.